Involvement of the transcription factor *E75* in adult cuticular formation in the red flour beetle *Tribolium castaneum*

Gelyn D. Sapin[a,1], Kai Tomoda[a], Sayumi Tanaka[a,2], Tetsuro Shinoda[b,c], Ken Miura[a] and Chieka Minakuchi[a,b*]

[a] Applied Entomology Laboratory, Graduate School of Bio-Agricultural Sciences, Nagoya University, Furocho, Chikusa, Nagoya 464-8601, Japan

[b] National Agriculture and Food Research Organization, 1-2 Ohwashi, Tsukuba 305-8634, Japan

[c] Faculty of Food and Agricultural Sciences, Fukushima University, 1 Kanayagawa, Fukushima 960-1296, Japan

* Corresponding author: Chieka Minakuchi, Dr. Agr.

Graduate school of Bio-Agricultural Sciences, Nagoya University, Nagoya 464-8601, Japan; Tel.: +81-52-789-4035; Fax: +81-52-789-4032; e-mail: c_mina@agr.nagoya-u.ac.jp

[1] Present address: Institute of Weed Science, Entomology and Plant Pathology, College of Agriculture and Food Science, University of the Philippines Los Baños, College, Laguna, 4031 Philippines

[2] Present address: Kyushu Okinawa Agricultural Research Center, National Agriculture and Food Research Organization, Koshi 861-1192, Japan

Abstract

Insect adult metamorphosis generally proceeds with undetectable levels of juvenile hormone (JH). In adult development of the red flour beetle *Tribolium castaneum*, biosynthesis of adult cuticle followed by its pigmentation and sclerotization occurs, and dark coloration of the cuticle becomes visible in pharate adults. Here, we examined the molecular mechanism of adult cuticular formation in more detail. We noticed that an exogenous JH mimic (JHM) treatment of Day 0 pupae did not inhibit pigmentation or sclerotization, but instead, induced precocious pigmentation of adult cuticle two days in advance. Quantitative RT-PCR analyses revealed that *ecdysone-induced protein 75B* (*E75*) is downregulated in JHM-treated pupae. Meanwhile, *tyrosine hydroxylase* (*Th*), an enzyme involved in cuticular pigmentation and sclerotization, was precociously induced, whereas a structural cuticular protein *CPR27* was downregulated, by exogenous JHM treatment. RNA interference-mediated knockdown of *E75* resulted in precocious adult cuticular pigmentation, which resembled the phenotype caused by JHM treatment. Notably, upregulation of *Th* as well as suppression of *CPR27* were observed with *E75* knockdown. Meanwhile, JHM treatment suppressed the expression of genes involved in melanin synthesis, such as *Yellow-y* and *Laccase 2*, but *E75* knockdown did not result in marked reduction in their expression. Taken together, these results provided insights into the regulatory mechanisms of adult cuticular formation; the transcription of genes involved in adult cuticular formation proceeds in a proper timing with undetectable JH, and exogenous JHM treatment disturbs their transcription. For some of these genes such as *Th* and *CPR27*, *E75* is involved in transcriptional regulation. This study shed light on the molecular mode of action of JHM as insecticides; exogenous JHM treatment disturbed the expression of genes involved in the adult cuticular formation, which resulted in lethality as pharate adults.

Keywords: Juvenile hormone, tanning, cuticle formation, E75, *Tribolium castaneum*, metamorphosis

1. Introduction

Metamorphosis is a change occurring in an insect from an immature stage to adult development (Belles 2020; Klowden, 2007). This change requires a coordination of changes in the several tissues and organs (Riddiford, 1996). On the other hand, molting is an occurrence that allows insects to grow and develop by shedding their old exoskeleton and generating a new one (Song et al., 2017). The insect exoskeleton is composed of cuticle and wax layers. Biosynthesis of adult cuticle followed by its tanning process (i.e. pigmentation and sclerotization) occurs during adult development. Genes encoding for enzymes involved in this process have been identified in the beetle *Tribolium castaneum* (reviewed in Noh et al., 2016). Tyrosine hydroxylase (Th) catalyzes the hydroxylation of tyrosine to 3,4-dihydroxyphenylalanine (dopa), and this is known to be the first step in pigmentation and sclerotization. Dopa decarboxylase (DDC) then converts dopa to dopamine. Catechols such as dopa, dopamine, and their derivatives such as *N*-β-alanyldopamine and *N*-acetyldopamine are oxidized to quinones or quinone methides by a phenoloxidase *Laccase2* (*Lac2*); these quinones are highly reactive cross-linking agents and indispensable to cuticular pigmentation and sclerotization (Arakane et al., 2005; Noh et al., 2016). The functions of genes involved in cuticular pigmentation and sclerotization have been analyzed by RNA interference (RNAi)-mediated knockdown in *T. castaneum*. Suppression of *Th* function decreased the hardness of the cuticle and decreased cuticular pigmentation (Gorman and Arakane, 2010). Knockdown of *DDC* resulted in lethal pupal phenotype with abnormal coloration, as well as delayed tanning of the adult cuticle (Gorman and Arakane, 2010). *T. castaneum* administered with dsRNA for *Lac2* resulted in failure of pigmentation and sclerotization in larval, pupal, and adult cuticles (Arakane et al., 2005). These studies suggested that *Th*, *DDC*, and *Lac2* are essential for cuticular pigmentation and sclerotization.

The primary components of the insect cuticle are chitin and cuticular proteins (CPs). In *T. castaneum*, at least three major CPs in the adult cuticle, namely *CPR4*, *CPR18*, and *CPR27*, have been identified and characterized (Arakane et al., 2012; Noh et al., 2014; Noh et al., 2015). Among these, *CPR18* and *CPR27* were identified as highly abundant CPs in elytra (Arakane et al., 2012), and are required for proper formation of the horizontal chitinous laminae and vertical pore canals in rigid cuticle (Noh et al., 2014), whereas *CPR4* is required for proper formation of the pore canals and pore canal fibers in rigid cuticle (Noh et al., 2015). These CPs have specific localization and cross-linking to particular CPs, which are critical in maintaining the exoskeleton morphology and

ultrastructure in beetles. In the case of *CPR27*, its transcript is localized in the elytra, pronotum, and ventral abdomen, which are highly sclerotized and hardened in mature adults (Arakane et al., 2012).

Insect molting and metamorphosis are under the control of the molting hormone (ecdysone) and juvenile hormone (JH) (reviewed in Belles 2020; Nijhout 1994; Riddiford et al., 2000). The former induces each molt during post-embryonic development, and the latter determines the nature of the molt. In the presence of abundant JH, insects repeat status quo (i.e. larva-larva) molts rather than undergoing metamorphosis precociously, whereas they undergo a metamorphic molt once the concentration of JH in the hemolymph decreases. Model insects such as the fruit fly *Drosophila melanogaster*, tobacco hornworm *Manduca sexta*, and red flour beetle *T. castaneum* have been utilized in understanding hormonal signaling cascades. Regarding the factors in the ecdysone signaling cascade, a number of ecdysone-response genes as well as an ecdysone receptor were identified first in the fruit fly by the early 1990s, and their homologs were subsequently found in other insect species. Meanwhile, JH receptor, a heterodimer of Methoprene-tolerant (Met) and Taiman (Tai) proteins, and an early JH-response gene *Krüppel homolog 1* (*Kr-h1*) were identified more recently (Li et al., 2011; Minakuchi et al., 2009; Minakuchi et al., 2008; Zhang et al., 2011; reviewed in Jindra et al., 2013; Riddiford et al., 2003).

Several transcription factors belonging to the nuclear receptor superfamily have been identified as mediators of hormonal signals. These nuclear receptors are defined by the presence of a highly conserved DNA-binding domain, and a less conserved C-terminal ligand-binding and dimerization domain (King-Jones and Thummel, 2005). In terms of biological functions, nuclear receptors are essential in growth, development, reproduction, homeostasis, and metabolism (Li et al., 2016; Reinking et al., 2005). The *ecdysone-induced protein 75B* (*E75*) is a nuclear receptor and known as one of the early response genes of 20-hydroxyecdysone (20E). As is often the case in nuclear receptors, *E75* has several isoforms that are generated by different promoters and through alternative splicing. *E75* isoforms have distinct roles in molting and metamorphosis. In the case of *D. melanogaster*, *E75A* mutants have reduced ecdysteroid titer in the larval stage followed by developmental arrest and molting defects, *E75B* mutants are viable, and *E75C* mutants die as adults (Bialecki et al., 2002). Three isoforms have been isolated in the silkworm *Bombyx mori*, and it was shown that *E75A* and *E75C* directly regulate the transcription of ecdysteroid biosynthetic genes (Li et al., 2016). In the German cockroach *Blattella germanica*, five *E75*

isoforms, with specific expression patterns and 20E responsiveness, were identified, and knockdown of all *E75* isoforms resulted in molting defects (Mané-Padrós et al., 2008).

Pupa-adult metamorphosis of holometabolous insects generally proceeds with an undetectable JH titer. In *T. castaneum*, topical application of JH mimic (JHM) to newly molted pupae inhibited pupa-adult metamorphosis and resulted in the formation of supernumerary or second pupae (Konopova and Jindra, 2007). *Kr-h1* expression is induced by exogenous JHM via Met-Tai complex (Jindra et al., 2015) and eventually causes upregulation of a pupal specifying transcription factor *broad* (*br*) (Konopova and Jindra, 2008; Minakuchi et al., 2009; Parthasarathy et al., 2008; Suzuki et al., 2008). Thus, *Kr-h1* and *br* mediate the status quo signals of JHM. Ureña et al. (2016) proposed the regulatory interactions in formation of adult development in *T. castaneum*: small amounts of JH in the prepupal stage caused up-regulation of *br* and suppression of the adult specifier *E93* via *Kr-h1*, whereas in adult development with undetectable JH, *E93* in turn represses the expression of *Kr-h1* and *br*, ensuring the completed transition of pupa to adult.

Extensive studies have been undertaken to elucidate the regulatory mechanisms of cuticular pigmentation and sclerotization in *M. sexta* (Hiruma and Riddiford, 2009). The transcription of *DDC*, the key enzyme in cuticular pigmentation and sclerotization, is regulated by 20E and JH (Hiruma and Riddiford, 2009). The ecdysone cascade leading to *DDC* transcription has been elucidated, in which 20E signals are mediated by its receptor (EcR-USP) and several ecdysone response genes, including *E75A*, *E75B*, *MHR3*, *MHR4*, and *βFTZ-F1* (reviewed in Hiruma and Riddiford, 2009). In addition, *DDC* activity was affected by the presence of JH (Hiruma et al., 1985). However, most of the regulatory mechanisms of cuticular pigmentation and sclerotization remain unknown.

In this study, we examined the expression of genes involved in adult cuticular formation in *T. castaneum*. Through quantitative RT-PCRs (qRT-PCRs) and hormonal treatment experiments, we revealed that the transcription factor *E75* was downregulated by the treatment of a JHM pyriproxyfen. Exogenous JHM treatment disturbed the transcription of several genes in adult cuticular formation, and among these, the transcription of *Th* and *CPR27* was regulated by *E75*.

2. Materials and Methods

2.1 Insects

The wild-type strain of *T. castaneum* was maintained in a rearing incubator in controlled conditions (dark and 30°C). The rearing procedure was followed based on the description by Yokoi et al. (2012).

2.2 Application of exogenous JH and JH mimics

JH III was kindly provided by Professor T. Shinada (Osaka City University), and was dissolved in n-hexane. Pyriproxyfen (Fujifilm Wako Pure Chemical), (*S*)-(+)-methoprene (Cayman Chemical Company), (*S*)-hydroprene (Sigma-Aldrich) and fenoxycarb (Fujifilm Wako Pure Chemical) were dissolved in methanol. Newly pupated test insects aged 0–12 h after pupation were aligned and adhered on a glass slide using double-sided tape. They were topically applied with either 0.4 μl of 0.1–3 mM pyriproxyfen (equivalent to 40 pmol–1.2 nmol: 12.9–386 ng), 0.4 μl of 0.1–1 mM (*S*)-(+)-methoprene (equivalent to 40 pmol–0.40 nmol: 12.4–124 ng), 0.4 μl of 0.1–1 mM (*S*)-hydroprene (equivalent to 40 pmol–0.40 nmol: 10.7–107 ng), 0.4 μl of 0.1–1 mM fenoxycarb (equivalent to 40 pmol–0.40 nmol: 12.1–121 ng), or 0.8 μl of 1 mM JH III (equivalent to 0.80 nmol: 213 ng), on the dorsal side of the abdomen. The same volume of the solvent was applied as a control. Six pupae were used for each treatment in the subsequent qRT-PCR study, and five to ten pupae were left for morphological observations. After treatment, pupae were transferred into a 24-well plate and stored in a rearing incubator.

2.3 cDNA cloning of *E75*

Partial sequences of *E75* were searched for in the BeetleBase (http://beetlebase.org; currently available as iBeetle-Base at http://ibeetle-base.uni-goettingen.de) and the DDBJ/EMBL-Bank/GenBank International Nucleotide Sequence Database. Based on the obtained sequences (Tc012440 from BeetleBase; XM_966269, XM_008199621, XM_008199622, and XM_008199623 from DDBJ/EMBL-Bank/GenBank Database), 5'RACE PCR was performed with a SMARTer RACE cDNA Amplification Kit (Takara Bio Inc.). Primer sequences are listed in Table S1. PCR products were subcloned into a pGEM-T Easy Vector Systems (Promega) and sequenced with a BigDye Terminator v3.1 Cycle Sequencing Kit (Thermo Fisher Scientific).

2.4 *E75* gene knockdown

The DNA template for dsRNA synthesis of *E75* was prepared by amplifying a DNA fragment containing a part of the target sequence with T7 promoter sequences on both ends. The primers used are listed in Table S1. These primers were designed in the common region of the five *E75* isoforms (Fig. S1). The PCR product was purified using a QIAquick PCR purification kit (Qiagen). After template preparation, dsRNA synthesis was done using a MEGAscript RNAi kit (Thermo Fisher Scientific) in accordance with the manufacturer's protocol. This was followed by dsRNA purification and ethanol precipitation.

Immobile and non-feeding final instar larvae were collected as prepupae. These prepupae were aligned on a glass slide using a double-sided tape with slight adhesiveness. Each prepupa was injected with 5 μg/μl of dsRNA solution (approximately 100 nl) using a fine glass needle prepared using a needle puller (Narishige) and glass capillary tubes (3.5" Drummond #3-000-203-G/X). The *maltose binding protein* (*malE*) dsRNA was used as a control treatment. The injected prepupae were transferred to a 24-well plate and stored in the rearing incubator.

2.5 Quantitative RT-PCR analysis

The transcript levels of selected genes were determined at different pupal ages using the whole body and legs of *T. castaneum*. Collection of staged pupae was commenced 24 h after application of 40 pmol of pyriproxyfen to newly molted pupae (equivalent to P1) or 24 h after dsRNA injection into prepupae (equivalent to P0). Sample collection was continued in 24 h interval until the pupae in the control treatment turned into adults. At 6 days after dsRNA injection, which was equivalent to P5, some individuals in the control treatment had already eclosed to adults, whereas others were still in the pupal stage. Thus, the age of this stage was designated as A0/P5. Three to six pupae were collected daily for each treatment, and each pupa or adult was homogenized with 200 μl TRIzol reagent (Thermo Fisher Scientific).

Total RNA was isolated from the whole body of each pupa or adult using TRIzol reagent. Another RNA isolation was done from the pooled pupal legs from three individuals. The isolated RNA was quantified using a spectrophotometer, and 500 ng of total RNA was used as the template for cDNA synthesis using whole pupal body, while 50–100 ng was used for legs. Following the manufacturer's protocol, genomic DNA elimination and cDNA syntheses were conducted using a PrimeScript RT reagent Kit with gDNA Eraser (Takara Bio Inc.).

Transcript levels of selected genes were determined using a Thermal Cycler Dice Real Time System (model TP800, Takara Bio Inc.). Each 14-µl mixture containing 1 µl of synthesized cDNA from a test insect, 7 µl of TB Green Premix Ex Taq (Takara Bio Inc.), 5.5 µl of nuclease-free water, and 0.28 µl of each forward and reverse primers. Primer sequences are listed in Table S1. The primers to quantify *E75*, *br*, *Kr-h1*, *HR3*, and *Ftz-f1* were designed in the common region among isoforms, while additional primer pairs to detect each isoform of *E75* were designed. The thermal cycling conditions were 95°C for 30 s, followed by 40 cycles of 95°C for 5 s and 60°C for 30 s. After thermal cycling, the absence of unwanted byproducts was confirmed by melting curve analysis. Regarding *E75* common region, *E75* isoforms, and *E93*, serial dilutions of a plasmid containing a part of the ORF of each gene were used as standards, and transcript levels were determined by absolute quantification. For other genes, the threshold cycle number for each transcript in the sample was determined based on the second derivative of its primary amplification curve by relative quantification. Transcript levels were normalized to that of *ribosomal protein L32* (*rpL32*) in the same sample.

2.6 Statistical analysis

All statistical analyses were done using GraphPad Prism (Version 8.2.1). An unpaired Student's *t*-test was done in comparing the means of treated and control treatments. The quantitative data were reported as mean ± standard error of the mean (SEM).

3. Results

3.1 Pupal morphology after exogenous JHM treatment

We first observed phenotypes after exogenous JHM treatment of newly molted pupae. We found that exogenous treatment with JHM at pupation caused precocious adult coloration in the epidermis (Fig. 1). Topical application of 40 pmol of pyriproxyfen caused dark coloration at P3, while cuticular coloration was not observed until P5 in pupae applied with solvent (Figs. 1A and 1B). In some of the pyriproxyfen-treated individuals, slippage of abdominal cuticle was observed at P3, but they never completed molting into adults and were arrested as pharate adults. The effect of pyriproxyfen treatment at different doses was examined. Increased dosage of pyriproxyfen (0.12,

0.40, and 1.2 nmol) resulted in similar phenotypes with variation from very light to dark coloration (Figs. 1E–1H). To observe the morphology of pyriproxyfen-treated pupae in more detail, the shedding pupal cuticle was removed using the tip glass microcapillary. A pupa-like new cuticle with a new set of pupal urogomphi and gin traps was formed on the abdomen (data not shown). By contrast, adult-like cuticular pigmentation was observed at P3 in pyriproxyfen-treated pupae, especially in legs (Figs. 1B, 1E-1H). Black pigmentation of hindwings, which generally occurs at P5 (Fig. 1A), was not observed at P5 after pyriproxyfen treatment (Fig. 1B).

In addition to using pyriproxyfen, JH III, and other JHM [fenoxycarb, (*S*)-hydroprene, and (*S*)-(+)-methoprene] were topically applied to newly molted pupae (Figs. 1C and 1I–1K). The morphology of pupae treated with 0.80 nmol of JH III had no significant difference from pupae treated with solvent until P4; reinduction of pupal characteristics such as pupal urogomphi and gin traps were not observed. However, they underwent incomplete ecdysis and finally arrested as pharate adults (Fig. 1C). By contrast, the morphology of pupae treated with fenoxycarb, (*S*)-hydroprene, and (*S*)-(+)-methoprene was similar to those in pyriproxyfen treatment (Figs. 1I–1K).

3.2 Expression profiles of the selected genes involved in metamorphosis and cuticular formation after exogenous JHM treatment

Expression profiles of genes involved in metamorphosis and cuticular formation were analyzed by qRT-PCR. We first analyzed the expression profiles of factors in hormonal signaling, i.e. *Kr-h1*, *br*, *E93*, *E75*, *HR3*, and *Ftz-f1*, using primers specific for their common regions (their expression profiles in normal pupae are shown in Figure S2). As expected, treatment with 40 pmol of pyriproxyfen upregulated both *Kr-h1* and *br*, and downregulated *E93* (Figs. 2A–2C). The expression levels of *E75* and *HR3* were significantly downregulated from P2 to P4, whereas *Ftz-f1* expression was not affected by treatment with 40 pmol of pyriproxyfen (Figs. 2D–2F). The expression profiles of the different *E75* isoforms were also determined using isoform-specific primers (Fig. S3A). Among the five isoforms, *E75B* and *E75E* were notably downregulated by pyriproxyfen treatment at P3 and P4; *E75A* was downregulated at P2; *E75C* was suppressed at P1; *E75D* was suppressed at P3.

The expression profiles of genes in adult cuticular formation were also examined. The expression of *Th* seemed to be precociously upregulated in pyriproxyfen-treated insects, but *Th*

expression was not significantly different compared with the control (Fig. 2G). The expression of *DDC* was slightly upregulated at P2 and P3, but significant downregulation was observed at P4 and P5 (Fig. 2H). The expressions of *Lac2* and *CPR27* were significantly decreased by pyriproxyfen treatment from P3 to P5 (Figs. 2I and 2J). As described above, the black pigmentation of hindwings was suppressed after pyriproxyfen treatment (Fig. 1B). Therefore, we examined the expression of *yellow-y* (*Y-y*), which is involved in melanin synthesis and important for black pigmentation of hindwings (Arakane et al., 2010), after pyriproxyfen treatment. The mean expression of *Y-y* was downregulated by pyriproxyfen treatment from P3 to P5, although not statistically significant at P3 (Fig. 2K).

As was observed in Figure 1, precocious adult cuticular tanning was evident especially in the mouthparts and legs, compared with other body parts such as the abdomen. Therefore, to further dissect the effect of pyriproxyfen treatment in inducing precocious adult cuticular tanning, the expression profiles of the selected genes were examined in the legs of *T. castaneum* at P3 to P5. As shown in Figure 3, upregulation of *Kr-h1* and *br* from P3 to P5, downregulation of *E93* at P5, and downregulation of *E75* at P3 and P4, were observed in the legs of pyriproxyfen-treated pupae (Figs. 3A–3D). A remarkable result was observed with *Th*, which showed significant upregulation at P3 and P4, and downregulation at P5, by pyriproxyfen treatment (Fig. 3E). The expression of *DDC* was downregulated in pyriproxyfen-treated pupae at P4 and P5 (Fig. 3F). For *Lac2*, significant downregulation was observed at P5 (Fig. 3G), and *CPR27* expression was completely suppressed by pyriproxyfen treatment at P3 and P4 (Fig. 3H). These observations were similar to the results using whole body pupae (Fig. 2).

3.3 Pupal morphology and gene expression profiles with *E75* knockdown

As stated above, exogenous JHM treatment of newly molted pupae resulted in downregulation of *E75*. To validate if *E75* is involved in the signaling, RNAi was performed by injecting dsRNA of an *E75* common region (ds*E75*) into prepupae. Evident dark coloration was observed in individuals administered with ds*E75*. This started to be noticed at P2 specifically on the mouthparts and legs (Fig. 4B). Over this period of time, the pupae treated with ds*E75* turned into a darker coloration and finally arrested as pharate adults. On the other hand, individuals

injected with ds*malE* had normal pupal coloration, and normally metamorphosed into adult after 5 days of pupal stage (Fig. 4A).

Expression profiles of the genes that are involved in hormonal signaling were quantified to unravel the possible reasons for pupal arrest and precocious tanning after *E75* knockdown. The expression of *Kr-h1* was upregulated from P2 to A0/P5, and there was a significant difference at A0/P5 (Fig. 5A). Meanwhile, *br* expression was not significantly affected from P0 to P4 (Fig. 5B). *E93* was slightly upregulated at P3 after *E75* knockdown (Fig. 5C). For *E75* gene, pupae that were administered ds*E75* showed slight upregulation at P1 and significant downregulation at P2 to P4 (Fig. 5D). The expression profiles of the different *E75* isoforms were also determined (Fig. S3B). In *E75* knockdown pupae, *E75B*, *E75C*, and *E75E* were upregulated in either P0 or P1, whereas *E75D* was suppressed at P0. On the other hand, significant downregulation was observed in either pupal ages from P2 to P4 in *E75A*, *E75B*, *E75D*, and *E75E*. In pupae after *E75* knockdown, the expression of *HR3* was significantly downregulated from P2 and P4, whereas *Ftz-f1* expression showed significant upregulation at P1 to P3 (Figs. 5E and 5F).

Expression profiles of the genes involved in cuticular formation were also examined after *E75* knockdown (Figs. 5G–5J). The expression of *Th* in *E75* RNAi pupae was upregulated from P1 to P4 to a statistically significant extent (Fig. 5G), which coincided with the downregulation of *E75* in pupae after *E75* knockdown (Fig. 5D). In the pupae that have been administered ds*E75*, the upregulation was also observed in *DDC* from P1 to P3, and at A0/P5 (Fig. 5H). Meanwhile, the expression of *Lac2* was not affected in pupae after *E75* knockdown except for P1, when a slight upregulation was observed (Fig. 5I). Lastly, the expression of *CPR27* was completely suppressed from P3 to A0/P5 (Fig. 5J). The expression of *Y-y* was also suppressed from P3 to A0/P5, although not statistically significant at P3 and A0/P5 (Fig. 5K).

Similar to the JHM study, the expression profiles of the selected genes after *E75* knockdown were examined in the legs of *T. castaneum* from P2 to P4 (Fig. 6). *Kr-h1* and *br* were upregulated at P2 and P3 in pupae after *E75* knockdown, and there was a significant difference in *br* transcript levels at P3 (Figs. 6A and 6B). *E93* was significantly upregulated at P3 and P4 after *E75* knockdown (Fig. 5C). As expected, significant downregulation of *E75* was observed in pupae after *E75* knockdown (Fig. 6D). *Th* and *DDC* expression levels were upregulated after *E75* knockdown, while the expression level of *Lac2* was not affected by *E75* knockdown (Figs. 6E–

6G). By contrast, *CPR27* was downregulated at P3 and P4 in the legs of the pupae injected with ds*E75* (Fig. 6H). Overall, the expression profiles of these genes in the legs were similar to those in the whole body (Fig. 5).

4. Discussion

In this study, we examined the molecular mechanism underlying adult cuticular formation. In *T. castaneum*, adult cuticular formation generally proceeds in the absence of endogenous JH. Therefore, we first examined the effects of an exogenous JHM treatment on adult cuticular formation. To our surprise, JHM treatment did not prevent or delay adult cuticular tanning, but instead, precocious pigmentation of the adult cuticle was observed in the mouthparts and legs. A similar observation was reported in the honeybee *Apis mellifera*, where topical application of the JHM pyriproxyfen resulted in precocious and enhanced pupal cuticle melanization (Bitondi et al., 1998; Zufelato et al., 2000). In this species, the involvement of 20E has also been suggested because injection of 20E at different doses suppressed cuticle pigmentation (Zufelato et al., 2000). Thus, exogenous JH and 20E had opposing effects in cuticle melanization in *A. mellifera*, but detailed hormonal signaling pathway has not yet been examined.

In our hands, JH III was less active compared with JHMs; JH III treatment did not cause reinduction of pupal characteristics (Fig. 1C). We think that this might be due to metabolic detoxification in *Tribolium* pupae: exogenous JH III might be metabolized more rapidly than synthetic JHMs. However, it will require further studies to verify this possibility. Konopova and Jindra previously reported that treatment with 0.3 mM JH III by dipping newly molted pupae was effective enough to induce the formation of second pupae (Konopova and Jindra, 2007). In our study, we topically applied a small amount of JH III (0.8 µl of 1 mM JH III); the difference in treating methods and doses might have caused discrepancy between these two studies.

Our qRT-PCR analysis revealed that JHM treatment affected the expression of known transcription factors in hormonal signaling in the adult development of *T. castaneum*. Both *E75* and *HR3* were downregulated by JHM treatment. In our preliminary experiments, RNAi-mediated knockdown of *E75*, but not *HR3* (data not shown), caused precocious adult cuticular pigmentation. Therefore, we focused on *E75* for further analysis. Notably, knockdown of *E75* in adult development caused a very similar phenotype to that after JHM treatment, i.e. adult cuticular

pigmentation approximately two days in advance. Through qRT-PCR analyses, we identified that *Th* is precociously upregulated, and this was more obvious when the transcript level was examined in legs only. *Th* encodes an enzyme that catalyzes the hydroxylation of tyrosine to dopa as the first step in pigmentation and sclerotization. Knockdown of *Th* in *T. castaneum* resulted in decreased hardness of cuticle as well as decreased cuticular pigmentation (Gorman and Arakane, 2010), indicating that *Th* is a key enzyme in cuticular tanning, and essential for normal adult development. Thus, our study provided a new insight that *Th* transcription is affected by JH levels, and *E75* is involved in the signaling.

The function of *Th* and *DDC* in melanin synthesis has been analyzed in larval black patterning of the butterfly *Papilio xuthus* (Futahashi and Fujiwara, 2008). The final instar larvae of *P. xuthus* have a cryptic green pattern, whereas younger larvae have a mimetic pattern of bird droppings with black coloration. Topical application of a JHM to penultimate instar larvae caused mimetic black patterning again, and changed the expression pattern of *Th* and *DDC* (Futahashi and Fujiwara, 2008), indicating that the transcription of *Th* and *DDC* is regulated by JH. Although the roles of *Th* and *DDC* are different between *P. xuthus* and *T. castaneum*, the transcriptional regulatory mechanism might be conserved to some extent.

We also found that *CPR27* encoding an adult cuticular protein was downregulated by JHM treatment or *E75* knockdown. This suggested that *CPR27* is generally expressed in adult development with undetectable levels of endogenous JH, and its transcription can be inhibited by JHM treatment. In addition, the metamorphosis-inhibiting signals of JHM to suppress *CPR27* are mediated by *E75*. *CPR27* is exclusively expressed during adult development, and its knockdown resulted in less rigid elytra (Arakane et al., 2012). In the mealworm beetle *Tenebrio molitor*, the cDNA sequence encoding an adult cuticular protein (ACP-22, named from the apparent molecular weight of 22 kDa on SDS-PAGE gels) has been identified, and treating pupae with the JHM methoprene caused supernumerary or second pupae, and suppressed *ACP-22* transcription (Bouhin et al., 1992). Thus, the mode of transcriptional regulation of adult cuticular protein may be similar among insect species.

We found that exogenous JHM treatment suppressed black pigmentation of hindwings, and the expression of genes involved in melanin synthesis, such as *Y-y* and *Lac2*, was downregulated (Figs. 1 and 2). This suggested that their transcription is normally maintained with undetectable endogenous JH, and exogenous JHM had an inhibitory effect on their transcription. These results

raised a possibility that the transcription of several genes in adult development is affected by JH levels. At present, we don't have any evidence that *E75* is involved in the transcription of *Y-y* and *Lac2* because our *E75* knockdown did not result in a marked reduction in their expression. Since *E75* knockdown caused reduction of *Y-y* transcripts at P4 (Fig. 5K), its transcription might be partly affected by *E75*.

The transcription factor *E75* has been identified in many insect species and functionally characterized in a couple of species, including the fruit fly *D. melanogaster* and the cockroach *B. germanica*. In *D. melanogaster*, most *E75A* mutants died with a prolonged second larval instar or were arrested during molting to the third larval instar; in addition, their ecdysteroid titers were reduced (Bialecki et al., 2002). In *B. germanica* nymphs, *E75* knockdown caused a precocious degeneration of the prothoracic glands, and an absence of ecdysteroid synthesis; consequently, they were unable to molt into adults (Mané-Padrós et al., 2008). Thus, *E75* has a role as a mediator of ecdysteroid signals, and a role in regulating ecdysteroid biosynthesis. In the meantime, there are several studies indicating that JH is also involved in regulating the transcription of *E75* in a stage-specific manner: for example, JH enhanced 20E-induced transcription of *E75A* in the final instar larvae of *M. sexta* (Zhou et al., 1998), whereas JH suppressed 20E-induced transcription of *E75C* in adult development (Keshan et al., 2006). Our study also showed that the transcript levels of *E75* in *T. castaneum* adult development were affected by JHM treatment (Figs. 2 and 3).

Regarding *E75* transcripts of *T. castaneum*, five isoforms generated by different promoters and alternative splicing were identified in publicly available database, and were also subcloned and sequenced by our 5'RACE PCR (Fig. S1). Our qRT-PCR analysis showed distinct developmental expression patterns among isoforms (Fig. S2). The transcript levels of *E75B*, *E75D*, and *E75E* were downregulated by JHM treatment (Fig. S3A), suggesting that these isoforms might be involved in signaling. Since we have not performed isoform-specific knockdown, the role of each *E75* isoform is still unknown in *T. castaneum*. Nevertheless, some of these isoforms may have redundant functions in adult development because the transcripts of all these isoforms are abundant at this stage. The expression profiles of the different *E75* isoforms in *E75* knockdown pupae were different among isoforms (Fig. S3B). This might be because the RNAi efficiency and timing of knockdown are diverse among isoforms.

Interestingly, some pupae that had been treated with a JHM exhibited slippage of abdominal cuticle at P3 (Fig. 1), although this was not observed when *E75* had been knocked down. However,

the mechanism how an exogenous JHM caused precocious cuticle slippage is unknown. One possibility could be that the exogenous JHM caused an increase in ecdysteroid titer, which resulted in precocious cuticle slippage and *Th* expression at P3 (Fig. 3E).

Based on our results, we hypothesized the regulatory mechanisms of adult cuticular formation (Fig. 7). In normal pupae in which endogenous JH is undetectable, the expression of *E75* is highly maintained at P2 and P3 (Figs. 2D, 5D, and S2D), which may induce adult cuticular formation by upregulating *CPR27* transcription at P3 and P4 (Figs. 2J, 5J, and S2J), and suppress precocious cuticular tanning by suppressing *Th* up to P4 (Figs. 2G, 5G, and S2G; Fig. 7A). When pupae were treated with an exogenous JHM, it suppressed the transcription of *E75* from P2 to P4 (Fig. 2D), which in turn may inhibit adult cuticle formation due to the suppression of *CPR27* transcription (Figs. 2J and 3H), and induce precocious cuticular tanning by upregulating *Th* (Figs. 2G and 3E; Fig. 7B). RNAi-mediated knockdown of *E75* caused similar effects and phenotypes to those after JHM treatment: precocious induction of *Th* and suppression of *CPR27* were observed (Figs. 5G and 5J; Fig. 7B). In the meantime, the transcriptions of *Y-y* and *Lac2* also occur with undetectable JH only, and JHM treatment downregulated their transcription (Figs 2K, 5K, and 7). However, this signaling is not mediated by *E75* (Fig. 7).

We found that not only *E75* but also *HR3* was downregulated by JHM treatment in adult development (Fig. 2). In this study, we did not do a further functional analysis of *HR3* because knockdown of *HR3* did not cause precocious adult cuticular pigmentation, although pupal lethality was also observed (data not shown). However, it is possible that *HR3* has an involvement in adult development besides adult cuticle formation. The role of *HR3* in *T. castaneum* larval stage was examined by Tan and Palli (2008), in which knockdown of *HR3* resulted in lethality as larvae. In the lepidopteran *Spodoptera litura*, JHM treatment upregulated *HR3* expression in adult females, suggesting that its expression is regulated by JH (Xu et al., 2015).

We have limited knowledge of whether *E75* is directly regulated by JH since this has not yet been examined. However, there is a possibility that JH or JHM regulates the transcription of *E75* in an indirect manner. One possibility is that JHM treatment decreased ecdysteroid titer by suppressing the expression of ecdysteroid biosynthetic genes, which in turn caused decreased mRNA levels of ecdysone-response genes such as *E75*. Further studies including promoter analysis of these genes will shed light on the regulatory mechanisms by hormones.

In general, JHMs such as pyriproxyfen are known to prevent adult development in a variety of insect species (Reviewed in Jindra and Bittova, 2020). Application of JHMs causes the reinduction of pupal characteristics, but in most cases, JHM-treated pupae are arrested without completing ecdysis. Our results indicated that an arrest as pharate adults is partly due to the disturbed expression of genes involved in adult cuticular formation including *Th*, *CPR27*, *Y-y*, and *Lac2*. We also suggested a possibility that JHM affected ecdysteroid titer, which resulted in incomplete molting. Thus, this study sheds light on the molecular mode of action of JHMs as insecticides.

Acknowledgments

We thank Dr. A. Miyanoshita (National Agriculture and Food Research Organization, Japan) for providing *T. castaneum*, and Dr. T. Shinada (Osaka City University) for providing JH III. C.M. was supported by a Grant-in-Aid for Japan Society for the Promotion of Science (JSPS) Fellows. Financial support for this research was also provided by JSPS KAKENHI Grant Number 15K07791 and 19H02969 to C.M.

References

Arakane, Y., Dittmer, N.T., Tomoyasu, Y., Kramer, K.J., Muthukrishnan, S., Beeman, R.W., Kanost, M.R., 2010. Identification, mRNA expression and functional analysis of several *yellow* family genes in *Tribolium castaneum*. Insect Biochem Mol Biol 40, 259-266. https://doi.org/10.1016/j.ibmb.2010.01.012.

Arakane, Y., Lomakin, J., Gehrke, S.H., Hiromasa, Y., Tomich, J.M., Muthukrishnan, S., Beeman, R.W., Kramer, K.J., Kanost, M.R., 2012. Formation of rigid, non-flight forewings (Elytra) of a beetle requires two major cuticular proteins. PLoS Genet. 8, e1002682. https://doi.org/10.1371/journal.pgen.1002682.

Arakane, Y., Muthukrishnan, S., Beeman, R.W., Kanost, M.R., Kramer, K.J., 2005. Laccase 2 is the phenoloxidase gene required for beetle cuticle tanning. Proc. Natl. Acad. Sci. U. S. A. 102, 11337–11342. https://doi.org/10.1073/pnas.0504982102.

Belles, X., 2020. Insect Metamorphosis. From Natural History to Regulation of Development and Evolution, 1st ed. Academic Press, London.

Bialecki, M., Shilton, A., Fichtenberg, C., Segraves, W.A., Thummel, C.S., 2002. Loss of the ecdysteroid-inducible E75A orphan nuclear receptor uncouples molting from metamorphosis in Drosophila. Dev. Cell 3, 209–220. https://doi.org/10.1016/S1534-5807(02)00204-6.

Bitondi, M.M.G., Mora, I.M., Simões, Z.L.P., Figueiredo, V.L.C., 1998. The Apis mellifera pupal melanization program is affected by treatment with a juvenile hormone analogue. J. Insect Physiol. 44, 499–507. https://doi.org/10.1016/S0022-1910(97)00113-3.

Bouhin, H., Charles, J.P., Quennedey, B., Delachambre, J., 1992. Developmental profiles of epidermal mRNAs during the pupal-adult molt of Tenebrio molitor and isolation of a cDNA clone encoding an adult cuticular protein: Effects of a juvenile hormone analogue. Dev. Biol. 149, 112–122. https://doi.org/10.1016/0012-1606(92)90268-L.

Futahashi, R., Fujiwara, H., 2008. Juvenile hormone regulates butterfly larval pattern switches. Science 319, 1061. https://doi.org/10.1126/science.1149786.

Gorman, M.J., Arakane, Y., 2010. Tyrosine hydroxylase is required for cuticle sclerotization and pigmentation in Tribolium castaneum. Insect Biochem. Mol. Biol. 40, 267–273. https://doi.org/10.1016/j.ibmb.2010.01.004.

Hiruma, K., Riddiford, L.M., 2009. The molecular mechanisms of cuticular melanization: The ecdysone cascade leading to dopa decarboxylase expression in Manduca sexta. Insect Biochem. Mol. Biol. 39, 245–253. https://doi.org/10.1016/j.ibmb.2009.01.008.

Hiruma, K., Riddiford, L.M., Hopkins, T.L., Morgan, T.D., 1985. Roles of dopa decarboxylase and phenoloxidase in the melanization of the tobacco hornworm and their control by 20-hydroxyecdysone. J. Comp. Physiol. B 155, 659–669. https://doi.org/10.1007/BF00694579.

Jindra, M., Bellés, X., Shinoda, T., 2015. Molecular basis of juvenile hormone signaling. Curr. Opin. Insect Sci. 11, 39–46. https://doi.org/10.1016/j.cois.2015.08.004.

Jindra, M., Bittova, L., 2020. The juvenile hormone receptor as a target of juvenoid "insect growth regulators". Arch Insect Biochem Physiol 103, e21615. https://doi.org/10.1002/arch.21615.

Jindra, M., Palli, S.R., Riddiford, L.M., 2013. The juvenile hormone signaling pathway in insect development. Annu. Rev. Entomol. 58, 181-204. https://doi.org/10.1146/annurev-ento-120811-153700.

509 Keshan, B., Hiruma, K., Riddiford, L.M., 2006. Developmental expression and hormonal
510 regulation of different isoforms of the transcription factor E75 in the tobacco hornworm
511 Manduca sexta. Dev. Biol. 295, 623–632. https://doi.org/10.1016/j.ydbio.2006.03.049.
512 King-Jones, K., Thummel, C.S., 2005. Nuclear receptors - A perspective from Drosophila. Nat.
513 Rev. Genet. 6, 311–323. https://doi.org/10.1038/nrg1581.
514 Klowden, M.J., 2007. Physiological Systems in Insects, 2nd ed. Academic Press, Massachusetts.
515 Konopova, B., Jindra, M., 2007. Juvenile hormone resistance gene *Methoprene-tolerant* controls
516 entry into metamorphosis in the beetle *Tribolium castaneum*. Proc. Natl. Acad. Sci. U. S. A.
517 104, 10488-10493.
518 Konopova, B., Jindra, M., 2008. Broad-Complex acts downstream of Met in juvenile hormone
519 signaling to coordinate primitive holometabolan metamorphosis. Development 135, 559–
520 568. https://doi.org/10.1242/dev.016097.
521 Li, M., Mead, E.A., Zhu, J., 2011. Heterodimer of two bHLH-PAS proteins mediates juvenile
522 hormone-induced gene expression. Proc. Natl. Acad. Sci. U. S. A. 108, 638-643.
523 https://doi.org/10.1073/pnas.1013914108.
524 Li, K., Tian, L., Guo, Z., Guo, S., Zhang, J., Gu, S.H., Palli, S.R., Cao, Y., Li, S., 2016. 20-
525 Hydroxyecdysone (20E) Primary Response Gene E75 isoforms mediate steroidogenesis
526 autoregulation and regulate developmental timing in bombyx. J. Biol. Chem. 291, 18163–
527 18175. https://doi.org/10.1074/jbc.M116.737072.
528 Mané-Padrós, D., Cruz, J., Vilaplana, L., Pascual, N., Bellés, X., Martín, D., 2008. The nuclear
529 hormone receptor BgE75 links molting and developmental progression in the direct-
530 developing insect Blattella germanica. Dev. Biol. 315, 147–160.
531 https://doi.org/10.1016/j.ydbio.2007.12.015.
532 Minakuchi, C., Namiki, T., Shinoda, T., 2009. Krüppel homolog 1, an early juvenile hormone-
533 response gene downstream of Methoprene-tolerant, mediates its anti-metamorphic action in
534 the red flour beetle Tribolium castaneum. Dev. Biol. 325, 341–350.
535 https://doi.org/10.1016/j.ydbio.2008.10.016.
536 Minakuchi, C., Zhou, X., Riddiford, L.M., 2008. *Krüppel homolog 1* (*Kr-h1*) mediates juvenile
537 hormone action during metamorphosis of *Drosophila melanogaster*. Mech. Dev. 125, 91-
538 105.
539 Nijhout, H.F., 1994. Insect Hormones. Princeton University Press, Princeton, New Jersey.

Noh, M.Y., Kramer, K.J., Muthukrishnan, S., Kanost, M.R., Beeman, R.W., Arakane, Y., 2014. Two major cuticular proteins are required for assembly of horizontal laminae and vertical pore canals in rigid cuticle of Tribolium castaneum. Insect Biochem. Mol. Biol. 53, 22–29. https://doi.org/10.1016/j.ibmb.2014.07.005.

Noh, M.Y., Muthukrishnan, S., Kramer, K.J., Arakane, Y., 2016. Cuticle formation and pigmentation in beetles. Curr. Opin. Insect Sci. 17, 1–9. https://doi.org/10.1016/j.cois.2016.05.004.

Noh, M.Y., Muthukrishnan, S., Kramer, K.J., Arakane, Y., 2015. Tribolium castaneum RR-1 Cuticular Protein TcCPR4 Is Required for Formation of Pore Canals in Rigid Cuticle. PLoS Genet. 11, e1004963. https://doi.org/10.1371/journal.pgen.1004963.

Parthasarathy, R., Tan, A., Bai, H., Palli, S.R., 2008. Transcription factor broad suppresses precocious development of adult structures during larval-pupal metamorphosis in the red flour beetle, Tribolium castaneum. Mech. Dev. 125, 299–313. https://doi.org/10.1016/j.mod.2007.11.001.

Reinking, J., Lam, M.M.S., Pardee, K., Sampson, H.M., Liu, S., Yang, P., Williams, S., White, W., Lajoie, G., Edwards, A., Krause, H.M., 2005. The Drosophila nuclear receptor E75 contains heme and is gas responsive. Cell 122, 195–207. https://doi.org/10.1016/j.cell.2005.07.005.

Riddiford, L.M., 1996. Molecular aspects of Juvenile Hormone Action in Insect Metamorphosis, in: Gilbert, L.I., Jamshed, R.T., Atkinson, B.G. (Eds.), Metamorphosis: postembryonic reprogramming of gene expression in amphibian and insect cells. Academic Press, San Diego, California, pp. 223–253.

Riddiford, L.M., Cherbas, P., Truman, J.W., 2000. Ecdysone Receptors and Their Biological Actions. Vitam. Horm. 60, 1–73.

Riddiford, L.M., Hiruma, K., Zhou, X., Nelson, C.A., 2003. Insights into the molecular basis of the hormonal control of molting and metamorphosis from *Manduca sexta* and *Drosophila melanogaster*. Insect Biochem Mol Biol 33, 1327-1338.

Song, Y., Villeneuve, D.L., Toyota, K., Iguchi, T., Tollefsen, K.E., 2017. Ecdysone Receptor Agonism Leading to Lethal Molting Disruption in Arthropods: Review and Adverse Outcome Pathway Development. Environ. Sci. Technol. 51, 4142–4157. https://doi.org/10.1021/acs.est.7b00480.

Suzuki, Y., Truman, J.W., Riddiford, L.M., 2008. The role of broad in the development of Tribolium castaneum: Implications for the evolution of the holometabolous insect pupa. Development 135, 569–577. https://doi.org/10.1242/dev.015263.

Tan, A., Palli, S.R., 2008. Edysone receptor isoforms play distinct roles in controlling molting and metamorphosis in the red flour beetle, Tribolium castaneum. Mol. Cell. Endocrinol. 291, 42–49. https://doi.org/10.1016/j.mce.2008.05.006.

Ureña, E., Chafino, S., Manjón, C., Franch-Marro, X., Martín, D., 2016. The Occurrence of the Holometabolous Pupal Stage Requires the Interaction between E93, Krüppel-Homolog 1 and Broad-Complex. PLoS Genet. 12, e1006020. https://doi.org/10.1371/journal.pgen.1006020.

Xu, Q., Tang, B., Zou, Q., Zheng, H., Liu, X., Wang, S., 2015. Effects of Pyriproxyfen on female reproduction in the common cutworm, Spodoptera litura (F.) (Lepidoptera: Noctuidae). PLoS One 10, e0138171. https://doi.org/10.1371/journal.pone.0138171.

Yokoi, K., Koyama, H., Minakuchi, C., Tanaka, T., Miura, K., 2012. Antimicrobial peptide gene induction, involvement of Toll and IMD pathways and defense against bacteria in the red flour beetle, Tribolium castaneum. Results Immunol. 2, 72–82. https://doi.org/10.1016/j.rinim.2012.03.002.

Zhang, Z., Xu, J., Sheng, Z., Sui, Y., Palli, S.R., 2011. Steroid receptor co-activator is required for juvenile hormone signal transduction through a bHLH-PAS transcription factor, methoprene tolerant. J. Biol. Chem. 286, 8437-8447. https://doi.org/10.1074/jbc.M110.191684.

Zhou, B., Hiruma, K., Jindra, M., Shinoda, T., Segraves, W.A., Malone, F., Riddiford, L.M., 1998. Regulation of the transcription factor E75 by 20-hydroxyecdysone and juvenile hormone in the epidermis of the tobacco hornworm, *Manduca sexta*, during larval molting and metamorphosis. Dev. Biol. 193, 127-138.

Zufelato, M.S., Bitondi, M.M.G., Simões, Z.L.P., Hartfelder, K., 2000. The juvenile hormone analog pyriproxyfen affects ecdysteroid-dependent cuticle melanization and shifts the pupal ecdysteroid peak in the honey bee (Apis mellifera). Arthropod Struct. Dev. 29, 111–119. https://doi.org/10.1016/S1467-8039(00)00023-2.

Figure legends

Figure 1. Phenotypes of *Tribolium castaneum* pupae that underwent topical application of JH or JHM. Newly molted pupae within 12 h after molting were treated with solvent, pyriproxyfen, or JH III. (A–C) Ventral view of pupae observed from pupa day 1 (P1) to pupa day 5 (P5) that had received the solvent methanol (A), 40 pmol pyriproxyfen (B), and 0.80 nmol of JH III (C). (D–K) Ventral view of pupae observed at P3 that had been treated with solvent (D), pyriproxyfen at 40 pmol (E), 0.12 nmol (F), 0.40 nmol (G), and 1.2 nmol (H), 0.40 nmol of fenoxycarb (I), 0.40 nmol of (*S*)-hydroprene (J), and 40 pmol of (*S*)-(+)-methoprene (K). The numerator is the number of phenotypes that were observed among the samples, and the denominator is the total number of test insects used in the experiment.

Figure 2. Expression profiles of selected genes in the whole body of *Tribolium castaneum* pupae after JHM treatment. Newly molted pupae within 12 h after molting were treated with 40 pmol of pyriproxyfen or an equal volume of solvent. RNA extraction from the whole body followed by quantitative RT-PCR were conducted at different pupal ages from pupa day 1 (P1) to pupa day 5 (P5). The transcript levels of *Kr-h1* (A), *br* (B), *E93* (C), *E75* (D), *HR3* (E), *Ftz-f1* (F), *Th* (G), *DDC* (H), *Lac2* (I), *CPR27* (J), and *Y-y* (K) were examined. Asterisks over the bars indicate statistically significant differences from the solvent-treated controls (*P≤0.05, **P≤0.01, ***P≤0.001, and ****P≤0.0001; Student's *t*-test). Means and standard errors of the mean (SEM) are shown (N=6). P-values are available in Table S2.

Figure 3. Expression profiles of selected genes in the legs of *Tribolium castaneum* pupae after JHM treatment. Newly molted pupae within 12 h after molting were treated with 40 pmol of pyriproxyfen or an equal volume of solvent. RNA extraction from pooled legs followed by quantitative RT-PCR were conducted from pupa day 3 (P3) to pupa day 5 (P5). The transcript levels of *Kr-h1* (A), *br* (B), *E93* (C), *E75* (D), *Th* (E), *DDC* (F), *Lac2* (G), and *CPR27* (H) were examined. Asterisks over the bars indicate statistically significant differences from the solvent-treated controls (*P≤0.05, **P≤0.01, ***P≤0.001, and ****P≤0.0001; Student's *t*-test). Means and standard errors of the mean (SEM) are shown (N=6). P-values are available in Table S3.

Figure 4. Ventral view of the *Tribolium castaneum* pupae and an adult that were treated with dsRNA of *malE* (A) and *E75* (B). The prepupae were injected with approximately 100 nl of 5 µg/µl dsRNA. P stands for pupa; A stands for adult; 0 to 5, day age; scale bars, 500 µm.

Figure 5. Expression profiles of selected genes in the whole body of *Tribolium castaneum* pupae and adults after *E75* knockdown. Prepupae were injected with dsRNA of *malE* or *E75*. RNA was extracted from the whole body, and quantitative RT-PCR was conducted from day 0 pupa (P0) to day 0 adult or day 5 pupa (A0/P5). The transcript levels of *Kr-h1* (A), *br* (B), *E93* (C), *E75* (D), *HR3* (E), *Ftz-f1* (F), *Th* (G), *DDC* (H), *Lac2* (I), *CPR27* (J), and *Y-y* (K) were examined. Inset of panel J shows the levels at A0/P5 by enlarging the Y-axis. Asterisks over the bars indicate statistically significant differences from the ds*malE*-treated controls (*P≤0.05, **P≤0.01, ***P≤0.001, and ****P≤0.0001; Student's *t*-test). Means and standard errors of the mean (SEM) are shown. Six samples each were used for P0 to P4, but only three samples were used for A0/P5. P-values are available in Table S4.

Figure 6. Expression profiles of selected genes in the legs of *Tribolium castaneum* pupae after *E75* knockdown. Prepupae were injected with dsRNA of *malE* or *E75*. RNA was extracted from the legs, and quantitative RT-PCR was conducted from P2 to P4. The transcript levels of *Kr-h1* (A), *br* (B), *E93*(C), *E75* (D), *Th* (E), *DDC* (F), *Lac2* (G), and *CPR27* (H) were examined. Asterisks over the bars indicate statistically significant differences from ds*malE*-treated controls (*P≤0.05, **P≤0.01, ***P≤0.001, and ****P≤0.0001; Student's *t*-test). Means and standard errors of the mean (SEM) are shown. Six samples each were used for P3 and P4, but only three samples were used for P2. P-values are available in Table S5.

Figure 7. A model for the regulatory pathway of adult cuticular formation in *Tribolium castaneum*. (A) In normal pupae with undetectable JH, *E75* induces adult cuticular formation in a proper timing; the expression of *CPR27*, *Y-y*, and *Lac2* is upregulated, and *Th* is suppressed. (B) In JHM-

or ds*E75*-treated pupae, *E75* was downregulated compared with normal pupae, which disturbed adult development of the cuticle; *CPR27*, *Y-y*, and *Lac2* were downregulated, and *Th* was induced precociously. *E75* is involved in regulating the transcription of *CPR27* and *Th*, but does not affect the transcription of *Y-y* or *Lac2*. See the Discussion section for details.

Supplementary Materials

Figure S1. The structure of *E75* isoforms of *Tribolium castaneum*.

Double-headed arrows represent the target region of quantitative RT-PCR primers, and the double underlines show the region of *E75* dsRNA. Arrowheads represent the position of the start codon in each isoform, and asterisks show the stop codon. Numbers in bars are length in bp.

Figure S2. Expression profiles of selected genes in whole body of *Tribolium castaneum* pupae and newly emerged adults.

RNA extraction from the whole body followed by quantitative RT-PCR were conducted at the different ages from pupa day 0 (P0) to adult day 0 (A0). Expression profiles of *Kr-h1* (A), *br* (B), *E93* (C), *E75* common region (D), *HR3* (E), *Ftz-f1* (F), *Th* (G), *DDC* (H), *Lac2* (I), *CPR27* (J), *Y-y* (K), *E75* isoforms (L–P) were examined. Means and standard errors of the mean (SEM) are shown (N=4).

Figure S3. Expression profiles of *E75* isoforms using whole body pupae of *Tribolium castaneum* after JHM treatment (A) and after *E75* knockdown (B).

(A) Expression profiles in the whole body of *Tribolium castaneum* pupae after JHM treatment. The same set of cDNAs as in Figure 2 was used. Newly molted pupae within 12 h after molting were treated with 40 pmol of pyriproxyfen or an equal volume of solvent. Asterisks over the bars indicate statistically significant differences from the solvent-treated controls (*$P \leq 0.05$, **$P \leq 0.01$, and ***$P \leq 0.001$; Student's *t*-test). Means and standard errors of the mean (SEM) are shown (N=6). P-values are available in Table S2.

(B) Expression profiles in the whole body of *Tribolium castaneum* pupae after *E75* knockdown. The same set of cDNAs as in Figure 5 was used. Prepupae were injected with dsRNA of *malE* or *E75*. RNA was extracted from the whole body, and quantitative RT-PCR was conducted. Asterisks over the bars indicate statistically significant differences from the ds*malE*-treated controls (*P≤0.05, **P≤0.01, ***P≤0.001, and ****P≤0.0001; Student's *t*-test). Means and standard errors of the mean (SEM) are shown. Six samples each were used for P0 to P4, but only three samples were used for A0/P5. P-values are available in Table S4.

Table S1 Primers used in this study.

Table S2 The P-values of the transcript levels of selected genes in the whole body of *Tribolium castaneum* pupae after treatment of 40 pmol of pyriproxyfen or solvent. The P-values indicating there is not statistically significant differences (P>0.05) are shadowed. The transcript levels are shown as graphs in Figure 2 and Figure S3.

Table S3 The P-values of the transcript levels of selected genes in the legs of *Tribolium castaneum* pupae after treatment of 40 pmol of pyriproxyfen or solvent. The P-values indicating there is not statistically significant differences (P>0.05) are shadowed. The transcript levels are shown as graphs in Figure 3.

Table S4 The P-values of the transcript levels of selected genes in the whole body of *Tribolium castaneum* pupae after injecting dsRNA of *malE* and *E75*. The P-values indicating there is not statistically significant differences (P>0.05) are shadowed. The transcript levels are shown as graphs in Figure 5 and Figure S3.

Table S5 The P-values of the transcript levels of selected genes in the legs of *Tribolium castaneum* pupae after injecting dsRNA of *malE* and *E75*. The P-values indicating there is not

713 statistically significant differences (P>0.05) are shadowed. The transcript levels are shown as
714 graphs in Figure 6.

715

716

Figure 1

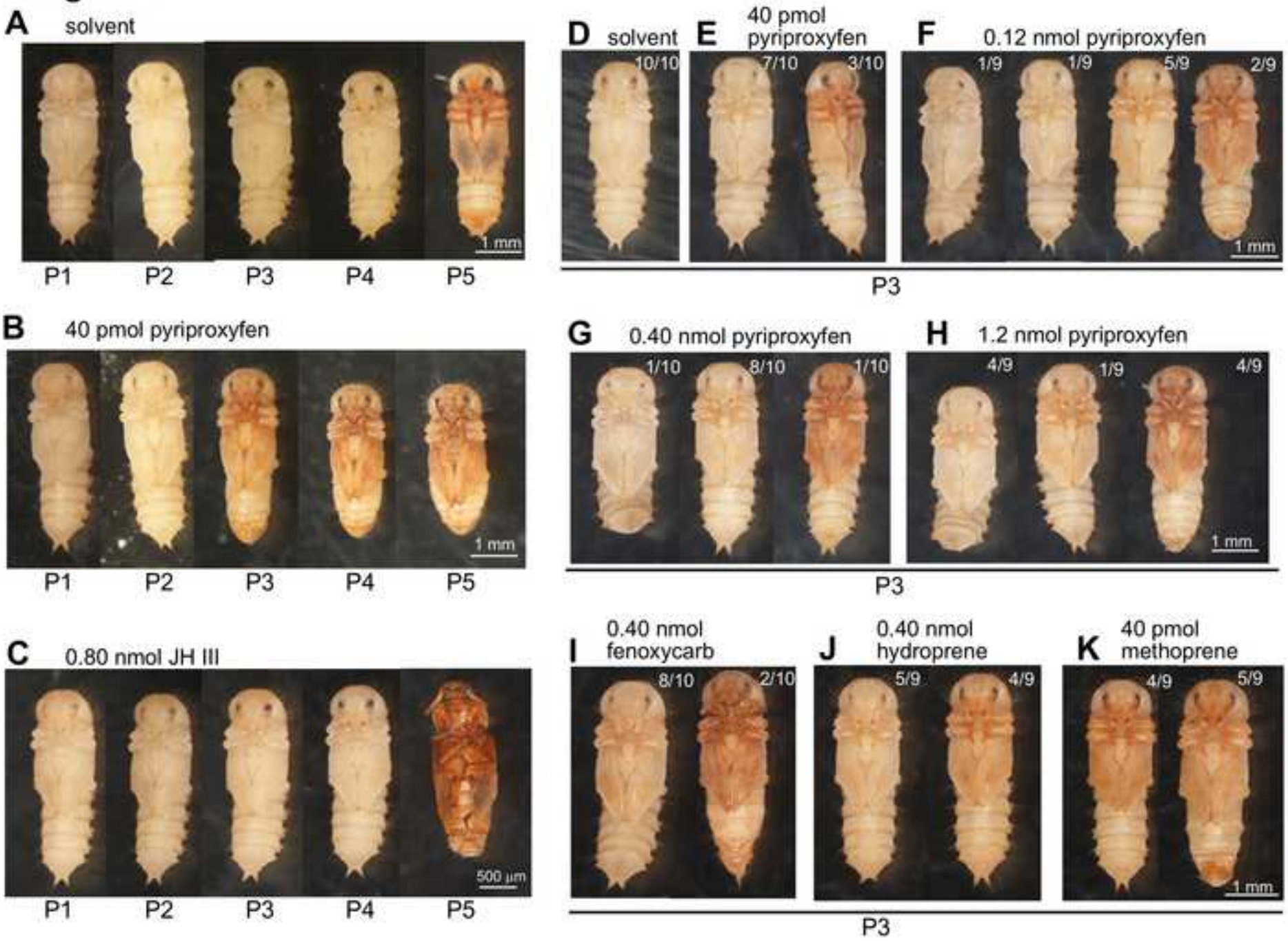

Figure 2

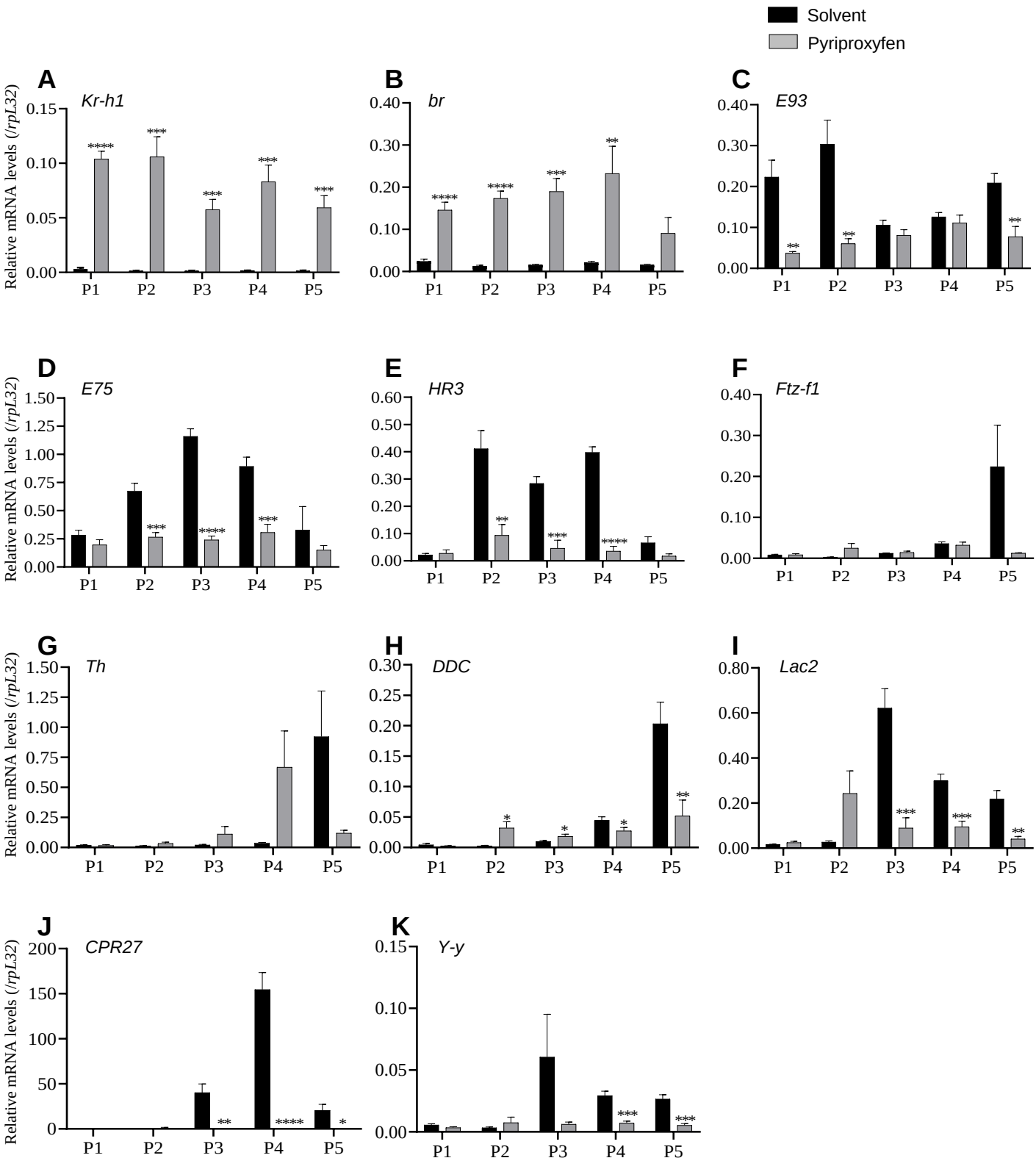
Solvent
Pyriproxyfen
A
Kr-h1
B
br
C
E93
D
E75
E
HR3
F
Ftz-f1
G
Th
H
DDC
I
Lac2
J
CPR27
K
Y-y
Relative mRNA levels (/rpL32)
P1
P2
P3
P4
P5

Figure 3

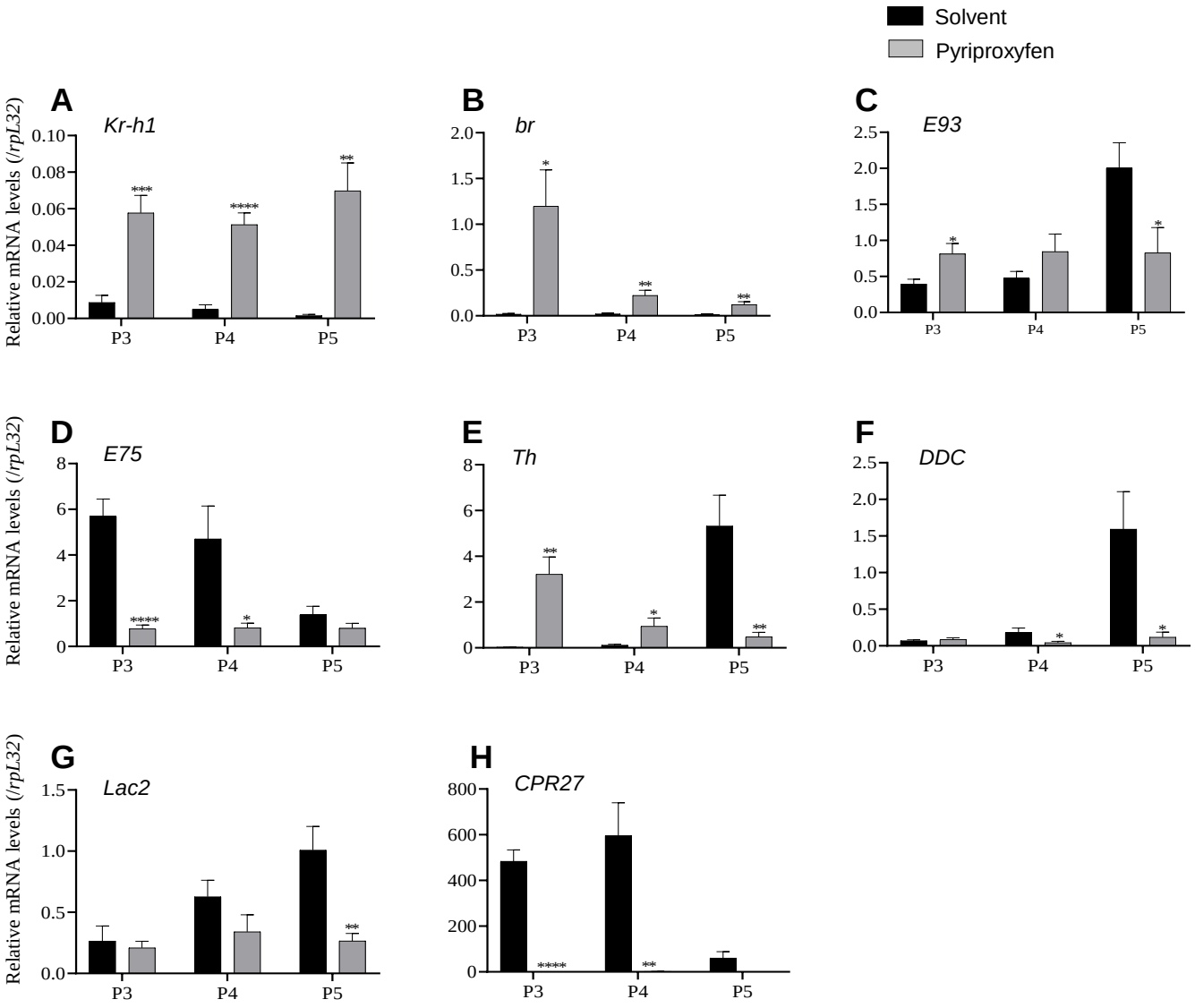
Solvent
Pyriproxyfen
A
Kr-h1
B
br
C
E93
D
E75
E
Th
F
DDC
G
Lac2
H
CPR27
Relative mRNA levels (/rpL32)
P3
P4
P5

Figure 4

A ds*malE*

B ds*E75*

Figure 5

Figure 5

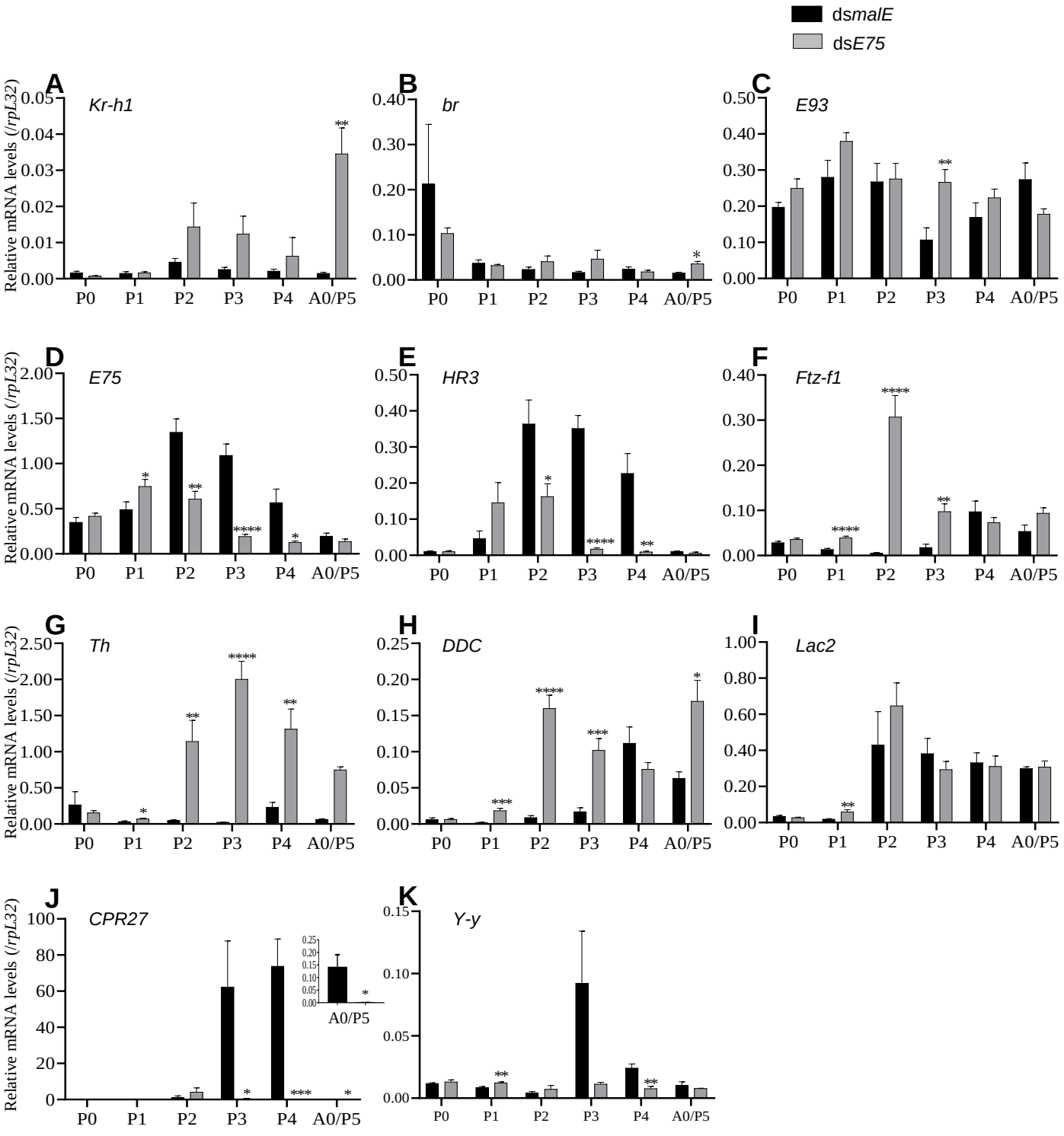

Figure 6

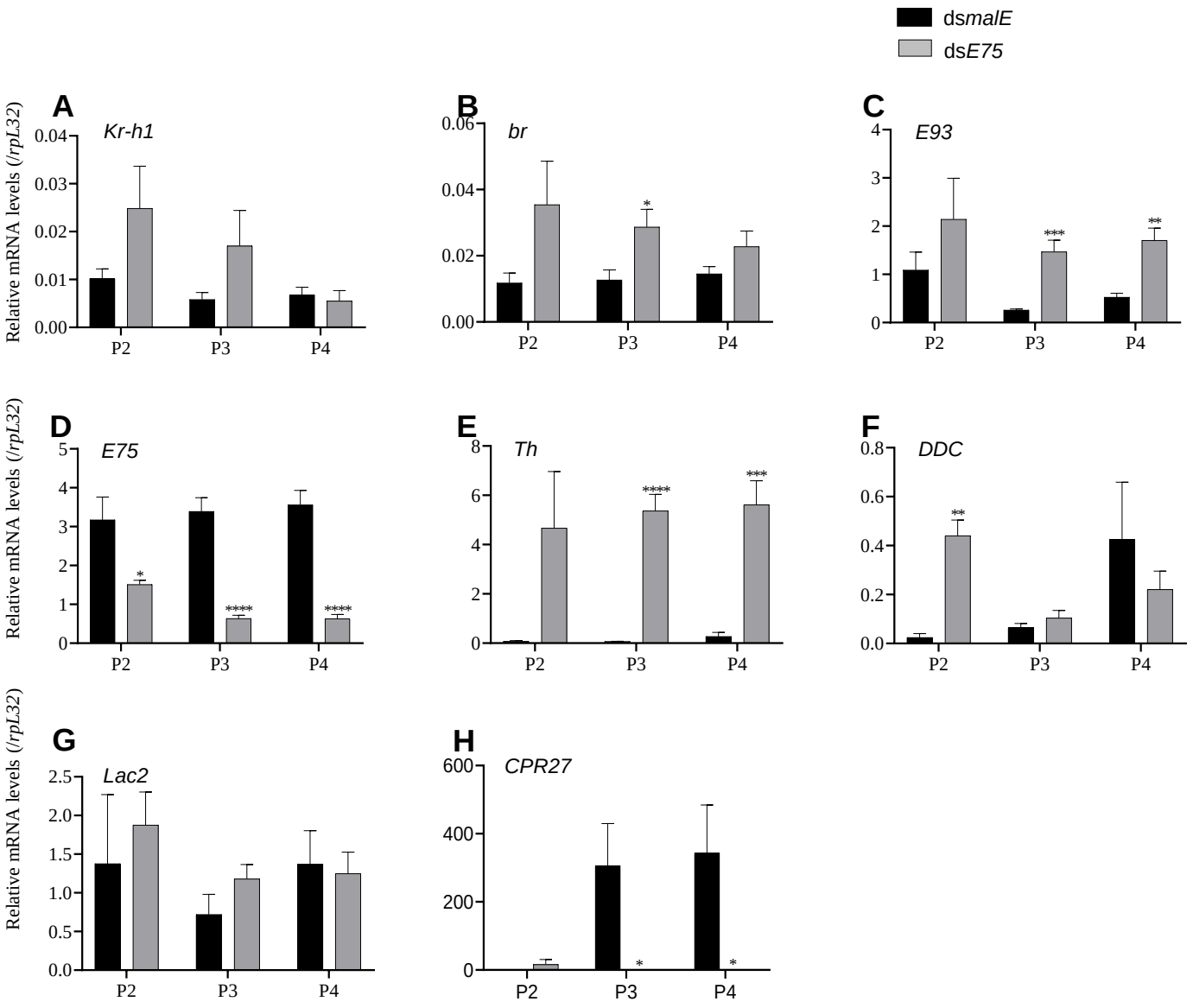
dsmalE
dsE75
A
Kr-h1
B
br
C
E93
D
E75
E
Th
F
DDC
G
Lac2
H
CPR27
Relative mRNA levels (/rpL32)
P2
P3
P4

Figure 7

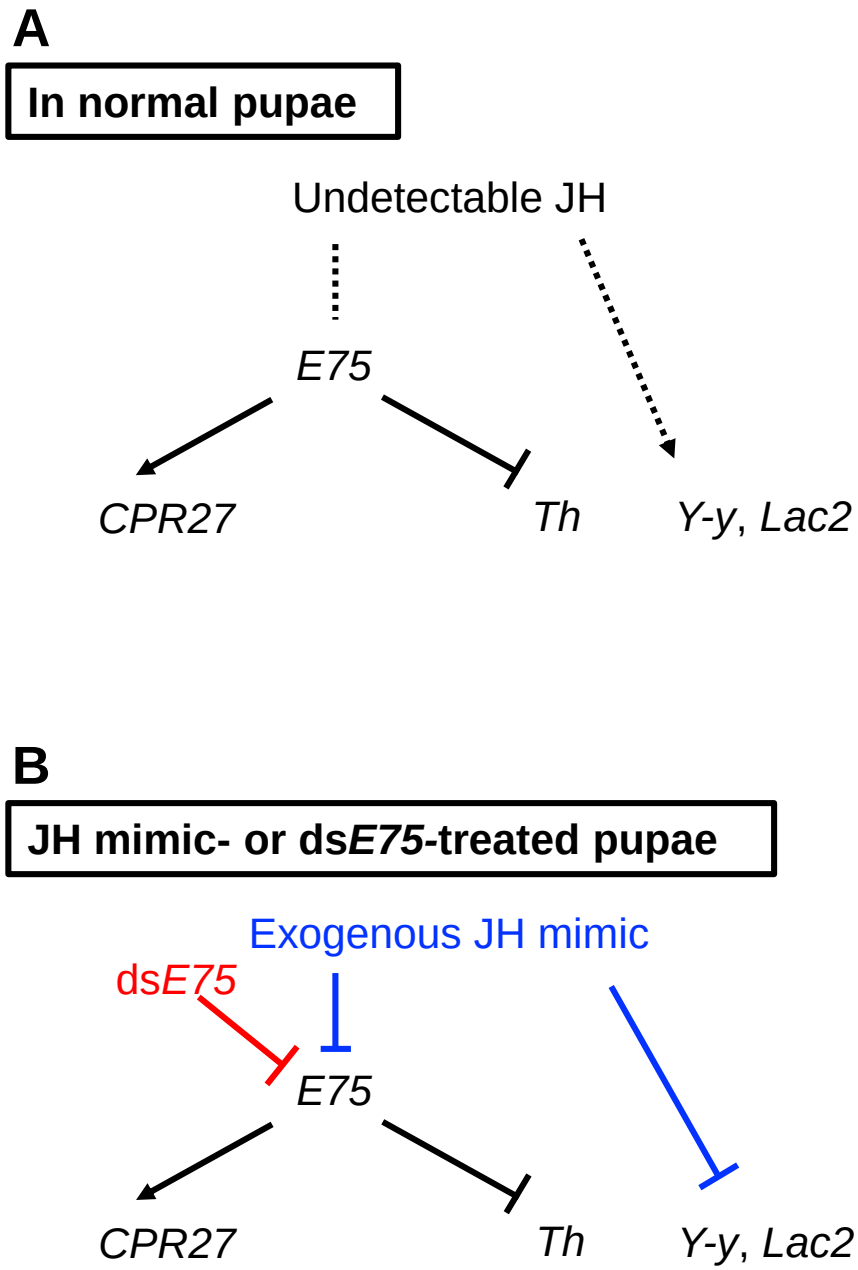
A
In normal pupae
Undetectable JH
E75
CPR27
Th
Y-y, Lac2
Observed phenotypes
Adult development of the cuticle in a proper timing
B
JH mimic- or dsE75-treated pupae
Exogenous JH mimic
dsE75
E75
CPR27
Th
Y-y, Lac2
Disturbed adult development of the cuticle

Table S1. Primers used in this study

Gene	Forward primer 5' to 3'	Reverse primer 5' to 3'
5'RACE PCR		
TcE75A-RR1	CGGTAATTGTCCACTGCTATCCGGTGA	
TcE75B-RR1	CATGTCAGGCGGCCACCATTGTTTAT	
TcE75C-RR1	ACTTGAACACGATGGTGGCGGTCTG	
TcE75D-RR1	TCACATGTGCACCAGCAGCACGATAG	
TcE75E-RR1	CGGTGGCACAGGTGGTCTCTTTGAA	
qRT-PCR		
E75 common	GCTTCATCATGGTCGTCCTCTT	AGGAGGTGATTTCTGAGGAGCA
E75A	CGGAATCCACCACGGATAGTAACA	AAGCCCTTGCATCCTTCGCA
E75B	GGCTCAGTGCTCCGTCGAATTT	GTTTTATCCGAACTCTGGGGCG
E75C	TAACGGGGGTGACGACATGCAG	TCCTCCTGCGTCTTGGGCTT
E75D	GACAGGCTATCGTGCTGCTGGT	GCTTTCTCCCTTTTCGGAACGC
E75E	GACAGCGAGAACCTCCTGGG	AGTGGACGCCGTAGTGGAA
E93	CTCTCGAAAACTCGGTTCTAAACA	TTTGGGTTTGGGTGCTGCCGAATT
br	CCAGCGGTCTCTTTCGTCGTTT	CGTCCTCCACTAACTTCTCGGTGAA
Kr-h1	TGCCATTGAATAACACCACCAA	CCAAGGGGTCTTCGGTGTAATA
HR3	GAACGACACGGGAAGCTTAATG	AAGTACGTGTGTGTGCGTCTGA
Ftz-f1	CTAACATCGTCGCCCGACTC	GAGCCCCAGAGCTTGTTGTC
JHAMT	CATCTCGCCCTATCACCATTCG	CCGCTGAAACCGATTTTGACAA
Tyrosine hydroxylase	CCAGACGCTGAAAAGGCTCT	TGACATACTGCCCCTTGGTG
DDC	TGAGGCTGGCCTTATTCCAT	GCAGCCAGATGTTGTTCGAG
Laccase 2	CGTTTTCAGGTGAACGATACGA	GTTGGTATGGCCCTTTGGCATA
Yellow-y	GGAAACACAACCCAAAACCCGT	TGGGTTTGTGTCTTCAGGTCGT
CPR27	GCCCAAGGGGGAGAAGGTTA	CTCCCATTGGTGGTGGAAGTC
rpL32	CAGGCACCAGTCTGACCGTTATG	GCTTCGTTTTGGCATTGGAGC
dsRNA synthesis (T7 promoter sequence is underlined)		
E75 common	TAATACGACTCACTATAGGGAAGTTCGAATTCGC GTTCTCTG	TAATACGACTCACTATAGGGATGAGTTCGGTGTT CCTCAAGC
HR3	TAATACGACTCACTATAGGGGAGATAATCCCGTG CAAAGTATGTG	TAATACGACTCACTATAGGGACGCTGTTGTACTG TCCACGTAATC

Table S2 The P-values of the transcript levels of selected genes in the whole body of *Tribolium castaneum* pupae after treatment of 40 pmol of pyriproxyfen or solvent. The P-values indicating there is not statistically significant differences (P>0.05) are shadowed. The transcript levels are shown as graphs in Figure 2 and Figure S3.

	P1	P2	P3	P4	P5
Kr-h1	<0.0001	0.0002	0.0001	0.0003	0.0004
br	<0.0001	<0.0001	0.0002	0.0086	0.0708
E93	0.0012	0.0024	0.1973	0.5080	0.0030
E75	0.1986	0.0005	<0.0001	0.0003	0.4209
HR3	0.6923	0.0021	0.0001	<0.0001	0.0644
Ftz-f1	0.8876	0.0780	0.6222	0.6959	0.0635
Th	0.8120	0.1340	0.1796	0.0619	0.0611
DDC	0.4892	0.0163	0.0470	0.0477	0.0064
Lac2	0.1615	0.0573	0.0003	0.0003	0.0010
CPR27	0.8639	0.2683	0.0020	<0.0001	0.0112
Y-y	0.1145	0.3757	0.1479	0.0002	0.0002
E75A	0.2638	0.0433	0.1553	0.9408	0.7730
E75B	0.2637	0.0756	0.0063	0.0041	0.3878
E75C	0.0152	0.0952	0.2040	0.4043	0.9252
E75D	0.8496	0.2027	0.0032	0.2284	0.6483
E75E	0.7043	0.4942	0.0002	0.0001	0.0675

Table S3 The P-values of the transcript levels of selected genes in the legs of *Tribolium castaneum* pupae after treatment of 40 pmol of pyriproxyfen or solvent. The P-values indicating there is not statistically significant differences (P>0.05) are shadowed. The transcript levels are shown as graphs in Figure 3.

	P3	P4	P5
Kr-h1	0.0008	<0.0001	0.0074
br	0.0139	0.0051	0.0073
E93	0.0254	0.1876	0.0385
E75	<0.0001	0.0235	0.1966
Th	0.0018	0.0466	0.0053
DDC	0.5783	0.0631	0.0171
Lac2	0.2018	0.1678	0.0045
CPR27	<0.0001	0.0020	0.0553

Table S4 The P-values of the transcript levels of selected genes in the whole body of *Tribolium castaneum* pupae after injecting dsRNA of *malE* and *E75*. The P-values indicating there is not statistically significant differences (P>0.05) are shadowed. The transcript levels are shown as graphs in Figure 5 and Figure S3.

	P0	P1	P2	P3	P4	P5/A0
Kr-h1	0.0782	0.7537	0.1743	0.0743	0.4346	0.0099
br	0.4246	0.4821	0.2117	0.1651	0.3393	0.0206
E93	0.0972	0.0866	0.9114	0.0082	0.2709	0.1178
E75	0.3038	0.0478	0.0015	<0.0001	0.0153	0.2425
HR3	0.9330	0.1279	0.0229	<0.0001	0.0028	0.1983
Ftz-f1	0.1135	<0.0001	<0.0001	0.0016	0.3723	0.0920
Th	0.5663	0.0180	0.0037	<0.0001	0.0035	0.1476
DDC	0.9037	0.0004	<0.0001	0.0006	0.1701	0.0243
Lac2	0.1992	0.0059	0.3549	0.3805	0.8006	0.7881
CPR27	0.6511	0.2243	0.2801	0.0368	0.0006	0.0481
Y-y	0.4952	0.0053	0.3929	0.0805	0.0012	0.3574
E75A	0.3625	0.2610	0.0639	0.0290	0.6250	0.3252
E75B	0.0015	<0.0001	0.0201	<0.0001	0.0331	0.5682
E75C	0.0323	0.0010	0.5047	0.1892	0.8929	0.1733
E75D	0.0172	0.0866	0.0007	0.0008	0.9339	0.0022
E75E	0.7539	0.0129	0.2266	0.0003	0.0012	0.6341

Table S5 The P-values of the transcript levels of selected genes in the legs of *Tribolium castaneum* pupae after injecting dsRNA of *malE* and *E75*. The P-values indicating there is not statistically significant differences (P>0.05) are shadowed. The transcript levels are shown as graphs in Figure 6.

	P2	P3	P4
Kr-h1	0.1787	0.1671	0.6509
br	0.1555	0.0271	0.1443
E93	0.3204	0.0006	0.0013
E75	0.0495	<0.0001	<0.0001
Th	0.1157	<0.0001	0.0003
DDC	0.0032	0.2917	0.4224
Lac2	0.6396	0.1811	0.8154
CPR27	0.3104	0.0327	0.0351

Figure S1

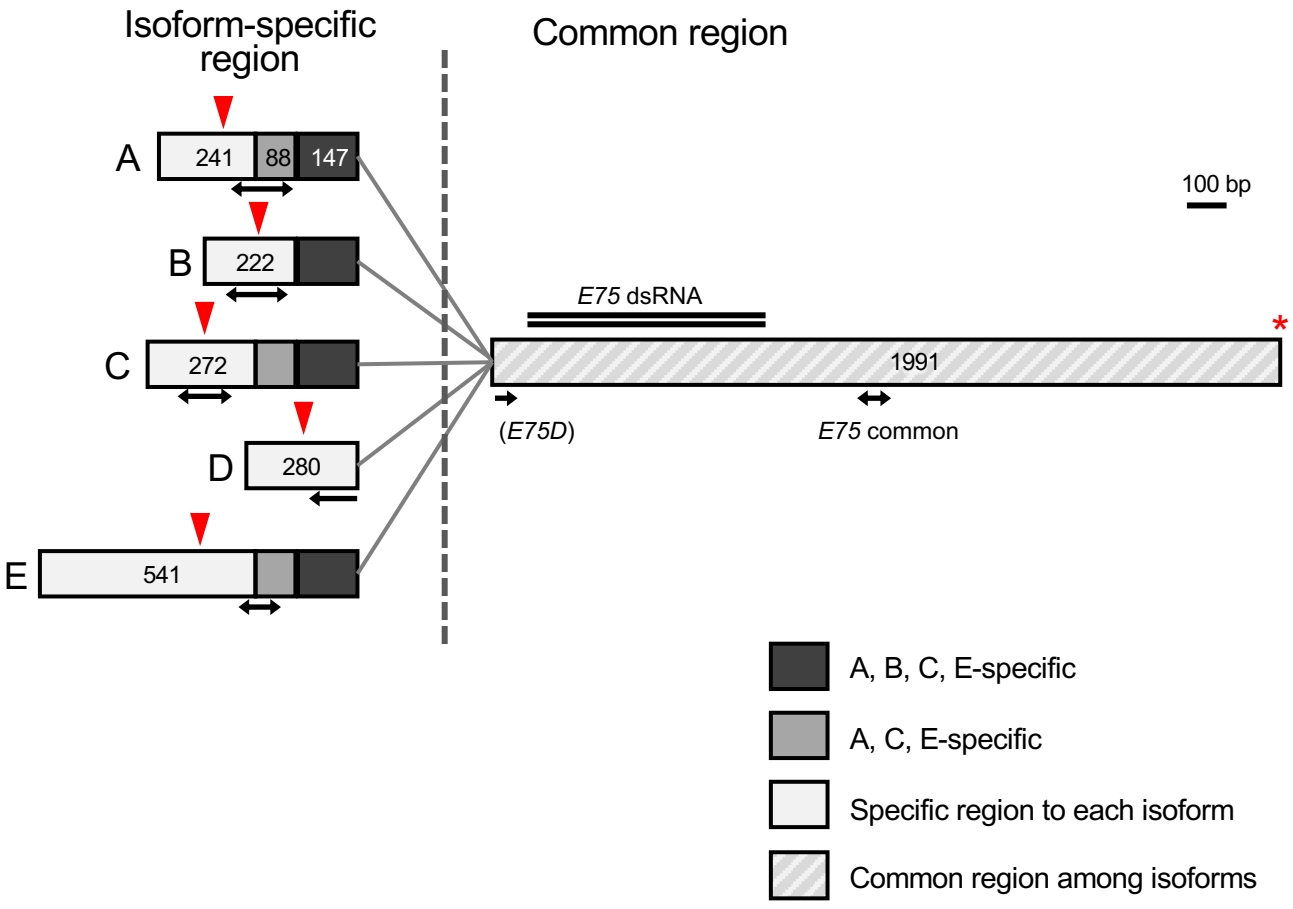
Isoform-specific region
Common region
A
241
88
147
B
222
C
272
D
280
E
541
100 bp
E75 dsRNA
1991
*
(E75D)
E75 common
A, B, C, E-specific
A, C, E-specific
Specific region to each isoform
Common region among isoforms

Figure S2

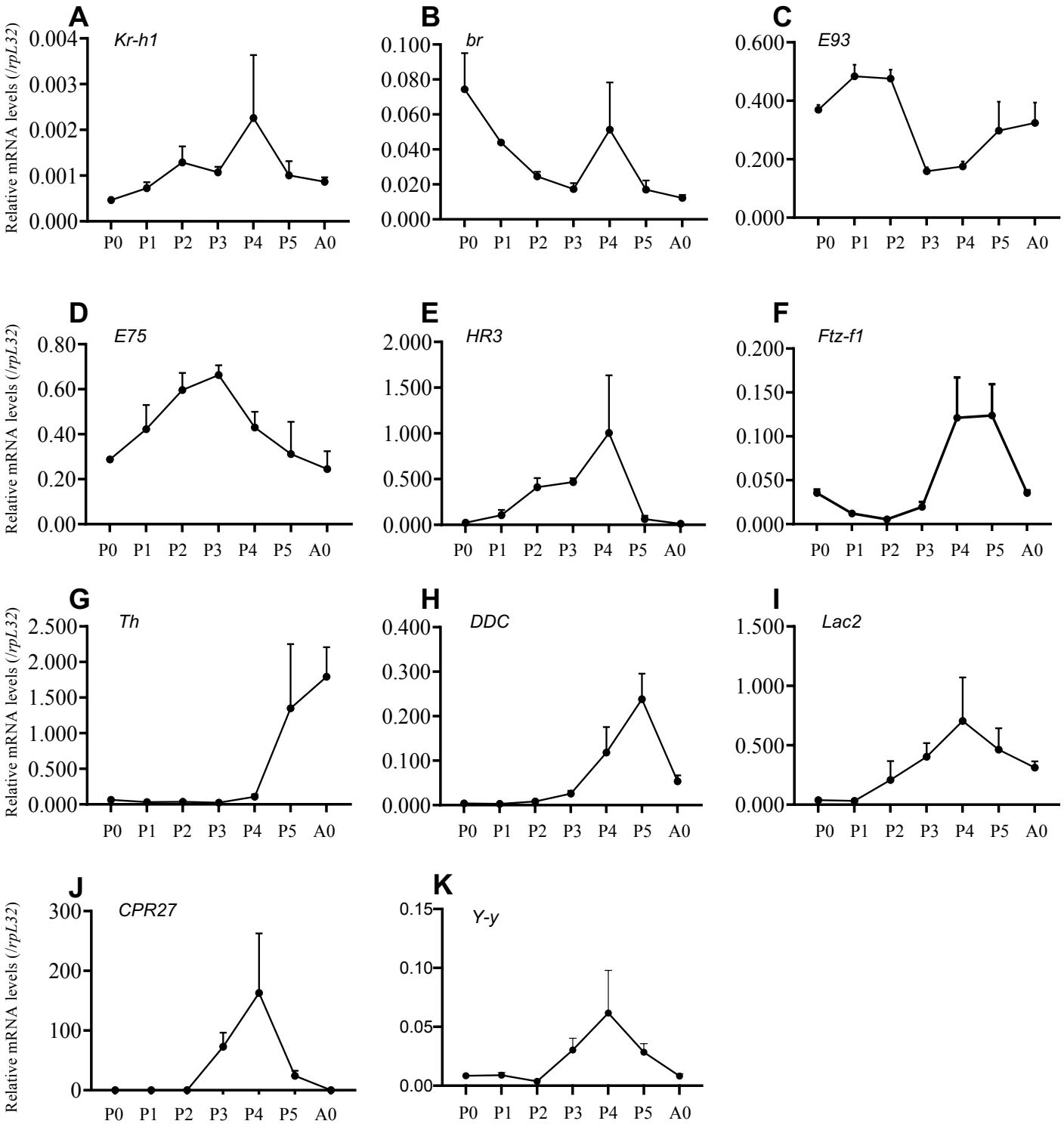
A
Kr-h1
B
br
C
E93
D
E75
E
HR3
F
Ftz-f1
G
Th
H
DDC
I
Lac2
J
CPR27
K
Y-y
Relative mRNA levels (/rpL32)
P0 P1 P2 P3 P4 P5 A0

Figure S2, continued

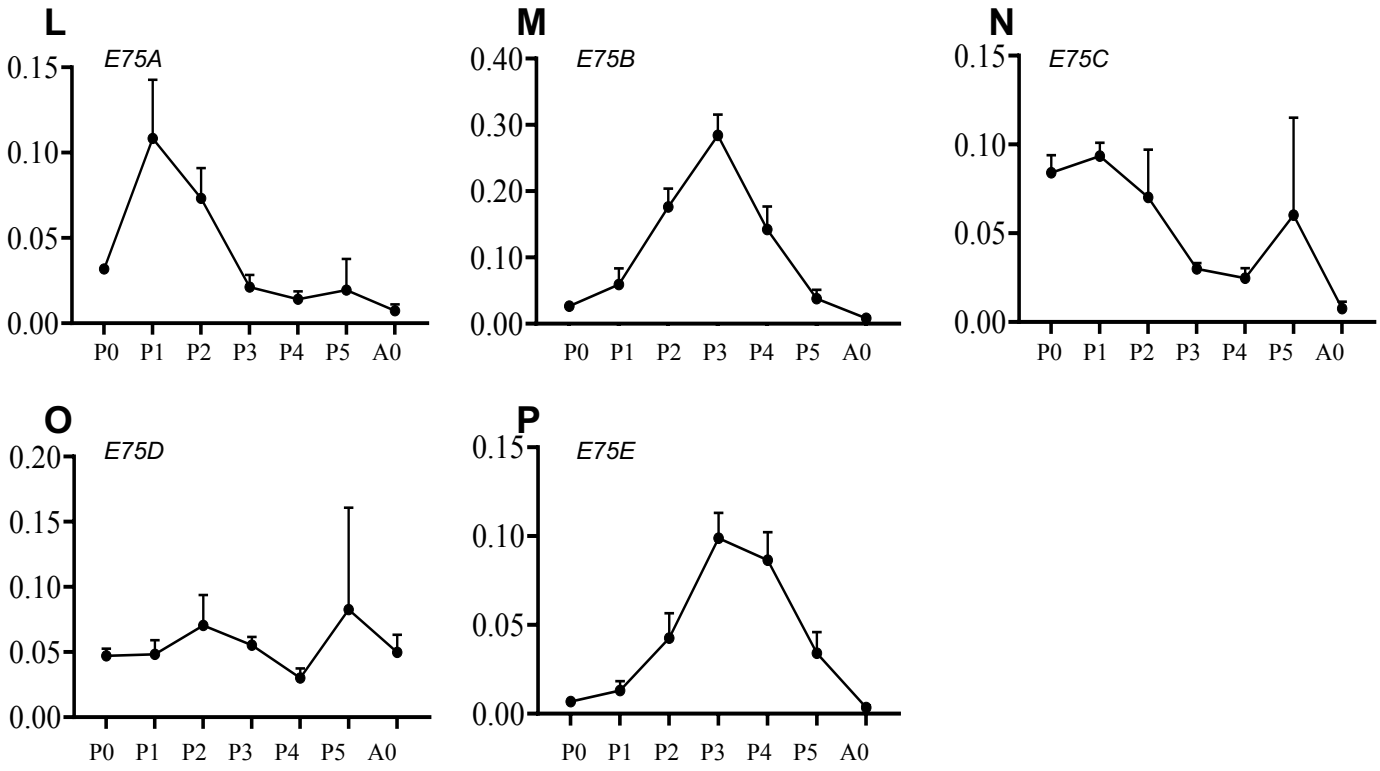

Figure S2

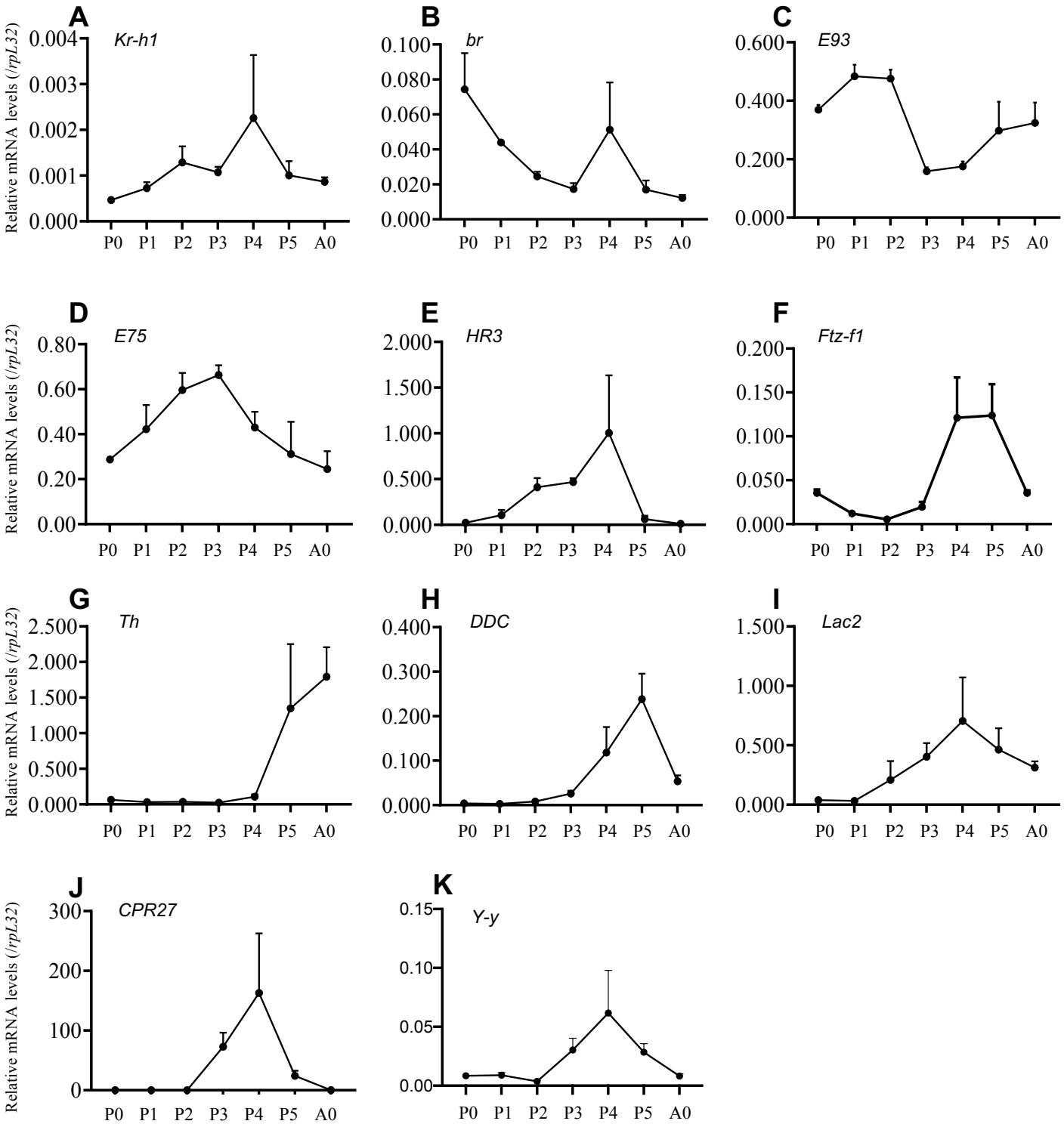
A
Kr-h1
B
br
C
E93
D
E75
E
HR3
F
Ftz-f1
G
Th
H
DDC
I
Lac2
J
CPR27
K
Y-y
Relative mRNA levels (/rpL32)
P0 P1 P2 P3 P4 P5 A0

Figure S2, continued